Soldagem & Inspeção

ISSN 1980-6973 (Online) | ISSN 0104-9224 (Print)
TECHNICAL PAPERS

Behaviors of Embrittlement and Softening in Heat Affected Zone of High Strength X90 Pipeline Steels

Yu Gu[1], Furen Xiao[2], Yongsheng Zhou[1], Jin Li[1], Caiyun Xu[1], Xiaodong Zhou[1]

[1] Zhoukou Normal University, School of Mechanical and Electrical Engineering, Zhoukou Henan, China.
[2] Yanshan University, College of Materials Science and Engineering, State Key Laboratory of Metastable Materials Science and Technology, Qinhuangdao Hebei, China.

How to cite: Gu Y, Xiao F, Zhou Y, Li J, Xu C, Zhou X. Behaviors of Embrittlement and Softening in Heat Affected Zone of High Strength X90 Pipeline Steels. Soldagem & Inspeção. 2019;24:e2415. https://doi.org/10.1590/0104-9224/SI24.15

Abstract: The embrittlement and softening behaviors in heat affected zone of X90 pipeline steel were studied, and the influence of weld thermal cycle on microstructure and mechanical properties were discussed by combining the effect of peak temperature on the phase transition point (Ar3). Results show that there are embrittlement and softening zones existed in heat affected zone of X90 pipeline steel. The peak temperature greatly affected the austenitizing and its grain size, thereby affected phase transition during cooling process. The embrittlement in critical heat affected zone at 750 °C was caused by brittle bainite and M /A islands formed during cooling, because little austenite was formed during heating. While, the embrittlement in coarse grain heat affected zone was caused by austenite grain coarsen, which transformed to the coarse bainite after cooling. The softening zone attributed to the polygonal ferrite and granular ferrite after cooling, which came from fine and ununiformed austenite formed during reheating process. Ar3 decreased with the increase of Cu, Cr or Mo content in steel, and the BF content in CGHAZ and GB and AF content in FGHAZ increased.

Key-words: Pipeline steel; HAZ; Mechanical property; Phase transition temperature; Chemical composition.

1. Introduction

In order to improve the transportation efficiency and reduce the transportation cost of oil and gas pipelines, pipeline transportation has been developed to large diameter and thick wall, and the requirements for the strength and toughness of pipeline steel are also becoming higher [1-4].To the turn of the century, large diameter (ϕ 1219/1422 mm), thick-walled X80 pipeline (t≥8.4 mm) has become a modern [5-9] choice for pipeline construction, such as the second and third west-east gas line in China, the central Asia gas pipeline, the Russia's ucha pipeline, and the China to Russia pipeline which is been built, etc. With the mature development of metallurgical technology, the development and research of the higher level X90-X120 pipeline steels are also promoted on the basis of X80 steel research and application. The large scale application of large diameter and thick wall X80 steel, accumulated lots of experience, and put forward the goal of development and construction the X90/100 test section, promoting the development of high strength steel pipe in all aspects.

In the production process of steel tube, the microstructure and mechanical properties in welding Heat Affected Zone (HAZ) change obviously due to the effect of welding thermal cycle, sequentially affect the operation security of pipeline significantly, then the embrittlement of HAZ has always been a focus in the study of pipeline steel [10-13]. However, in the study of X80 steel, we found that not only the embrittlement phenomenon exists in the HAZ, but also occurs softening phenomenon caused by strength reduced sharply [14,15], and the softening affects the fatigue strength seriously, hence affects the operation security of pipeline. With the increase of the strength of pipeline steel and the increase of wall thickness of steel pipe, the softening of HAZ may be more serious. Therefore, the study on high-strength pipeline steel should not only pay attention to the embrittlement, but also to the softening of the welding heat affected zone.

In this work, six typical X90 steels were selected, thermal simulation has been used to study the effects of peak temperature on microstructure and properties in heat affected zone in X90 steels, meanwhile, the relationship between composition, microstructure and performance is discussed combined with the phase transformation due to welding thermal cycle in this work. These results provide an experimental basis for understanding the evolution of the microstructure and performance of the heat affected zone, as well as the control of the microstructure and performance.

Received: 19 Mar., 2019. Accepted: 20 June, 2019.
E-mails: 202guyu@163.com (YG), frxiao@ysu.edu.cn (FX), 270353531@qq.com (YZ), lijin309@126.com (JL), xu_caiyun@126.com (CX), zhouxd516@163.com (XZ)

2. Material and Methods

Test pieces were cut from the central section of commercial API X90 steel plates, the chemical compositions are shown in Table 1. In which, the content of Cu (Steel A and Steel B), Cr (Steel C and Steel D) and Mo (Steel E and Steel F) were chosen as examples to discuss the effect of alloy composition of X90 steel on HAZ.

Table 1. Chemical composition of the test steels (wt.%).

	C	Si	Mn	P	Cr	Mo	Ni	Al	Cu	Nb	Ti	Ceq
A	0.06	0.22	1.65	0.010	0.23	0.01	0.219	0.036	0.019	0.079	0.016	0.39
B	0.06	0.23	1.64	0.007	0.22	0.01	0.221	0.035	0.139	0.079	0.017	0.40
C	0.05	0.24	1.78	0.012	0.01	0.12	0.180	0.038	0.009	0.059	0.015	0.40
D	0.06	0.22	1.79	0.009	0.29	0.13	0.150	0.041	0.012	0.062	0.016	0.45
E	0.06	0.28	1.81	0.009	0.23	0.22	0.185	0.027	0.236	0.092	0.013	0.48
F	0.05	0.26	1.77	0.008	0.23	0.30	0.231	0.033	0.234	0.090	0.014	0.48

The welding thermal simulation experiments were carried out on a Gleeble 3500 thermal-mechanical simulator. The simulation parameters are determined according to the actual welding heat input of four wire submerged arc welding in steel pipes. The peak temperatures of 1350, 1200, 1000, 900, 800, 750, 700, 650 °C were selected to simulate the reheated HAZ from CGHAZ region to the sub-intercritically reheated region. And the specimens were uniformly and rapidly heated up at a rate of 150 °C/s to different peak temperatures and held for 1 s. The cooling time from 800 °C to 300 °C is 53 s. The expansion curve was measured by means of expansion method for the round specimens, and the phase transition temperature of cooling process was determined. After simulation, the round specimens and the cuboid specimens were further machined into standard tensile and Charpy V-notch samples, respectively. Some type specimens after thermal cycle were selected for microstructure observation. The microstructure observations were conducted using optical microscopy, scanning electron microscope (SEM) and transmission electron microscopy (TEM).

3. Results and Discussion

3.1. Effect of peak temperature on mechanical property

Figure 1 shows mechanical properties of six steels after reheat at different peak temperatures. Figure 1 shows that within the peak temperature range in this experiment, the strength and toughness show an opposite trend with the decrease of the peak temperature.

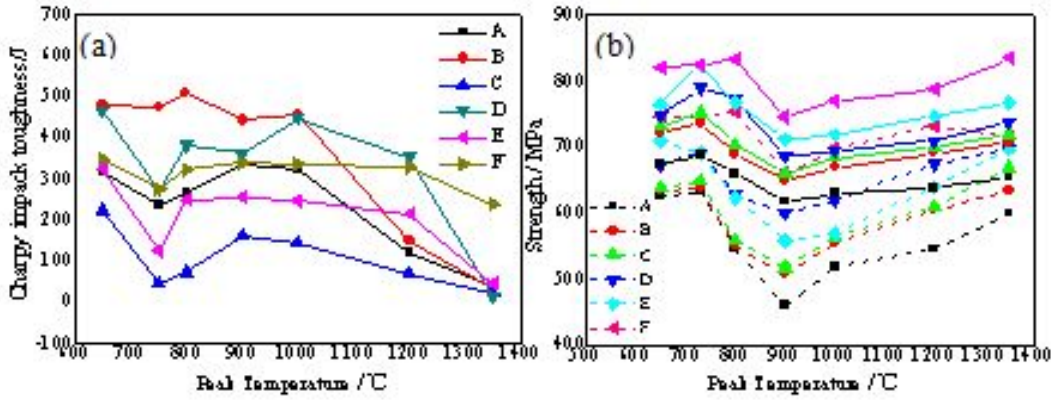

Figure 1. Mechanical properties of the test steels at different simulated peak temperature: (a) toughness; (b) strength.

For Steel C, as an example, when the peak temperature is 1350 °C, the steel mantains high strength, but the impact toughness is very low, only about 20 J. With the decrease of peak temperature, the strength become lower but the impact toughness become higher, then the strength and toughness obtain extreme values at 900 °C and 1000 °C, respectively. The yield strength decreases to less than 650 MPa, however, the impact toughness rises to about 200 J. As the peak temperature decreases further, the strength increases but the impact toughness decreases. When the peak temperature decrease to 750 °C, the strength up to the maximum, the impact toughness approaches to the minimum, which is only about 50 J. As the peak temperature decrease to 700 °C, the strength has little change, but the impact toughness significantly rises to about 250 J. When the peak temperature decreases further, the strength and toughness decreases slightly, but not much. In addition, according to the change rule of strength with the peak temperature, the yield strength decreases more than the tensile strength, so the yield ratio decreases. This change is related to the difference of microstructure obtained at different peak temperature. The evolutions of strength and toughness with the peak temperature of other steels are similar to that of Steel C. It indicates that, meanwhile, for the toughness and strength, Steel A is lower than Steel B, Steel C is lower than Steel D, Steel E is lower than Steel F, which means, the increase of Cu, Cr or Mo content in steel can improve the mechanical property in the HAZ.

3.2. Effect of peak temperature on microstructure

For the low-carbon microalloyed steels, in order to identify the microstructure, the classified method proposed in Yue [12] and Kumar et al. [13] was used in this work, i.e., the microstructure is classified as polygonal ferrite (PF), quasi-polygonal ferrite (QF or massive ferrite MF), granular bainite (GB), bainite ferrite (BF), which is summarized in Table 2.

The microstructures of the base metals are shown in Figure 2. Figure 2 indicates that six test steels are in obvious rolling state, and the constitutes of microstructure are similar, all of which are composed of a large number AF and a small number of polygons ferrite PF and QF. The test pieces were machined into round specimens of φ10×100 mm and cuboid specimens of 10×10×80 mm for HAZ simulation, and used to determine the strength and impact toughness after welding thermal simulation, respectively.

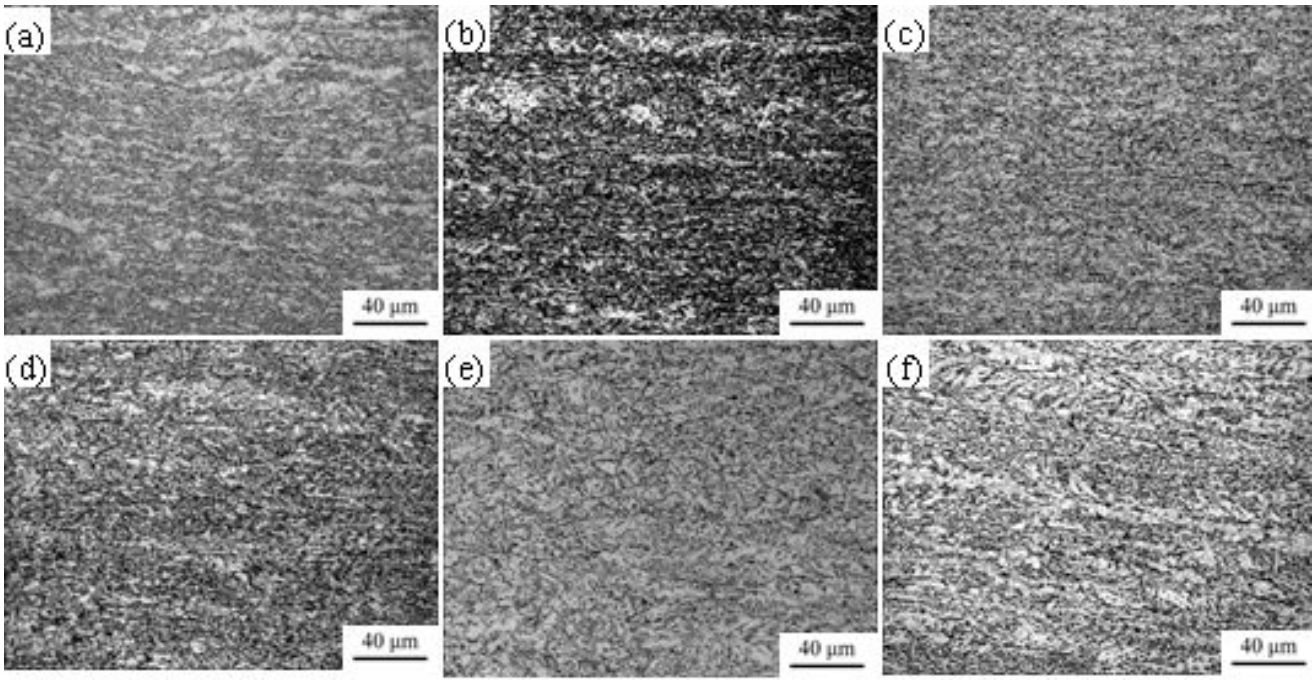

Figure 2. Optical metallographs of the base metal: (a) Steel A; (b) Steel B; (c) Steel C; (d) Steel D; (e) Steel E; (f) Steel F.

Figures 3 and 4 show typical optical microstructures of steel A after reheat at different peak temperatures, Figure 5 shows typical optical microstructures of steel B-F after reheat at different peak temperatures.

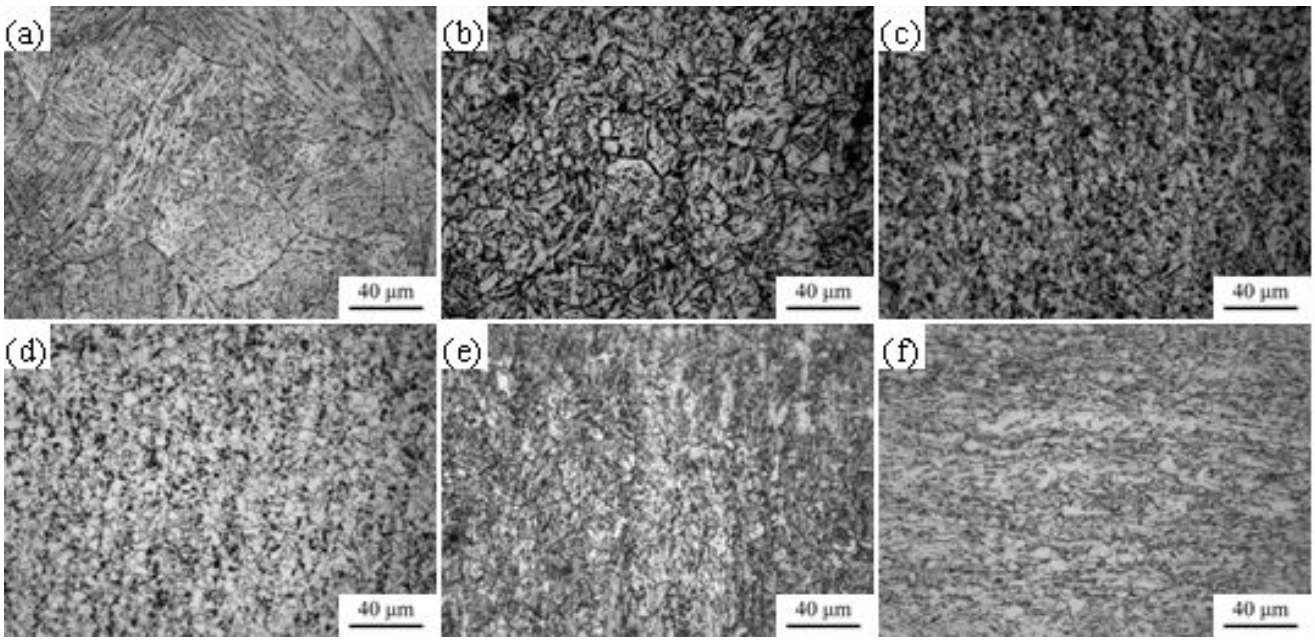

Figure 3. Optical metallographs of steel A at different simulated peak temperature: (a) 1350 °C; (b) 1200 °C; (c) 1000 °C; (d) 900 °C; (e) 800 °C; (f) 750 °C.

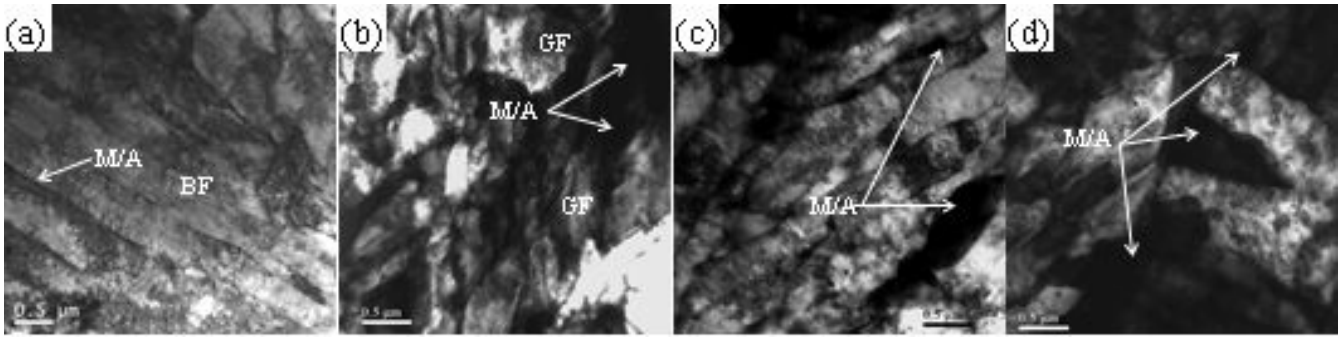

Figure 4. TEM of M/A island constituent at different simulated peak temperature of steel A: (a) 1350 °C; (b) 900 °C; (c) 800 °C; (d) 730 °C.

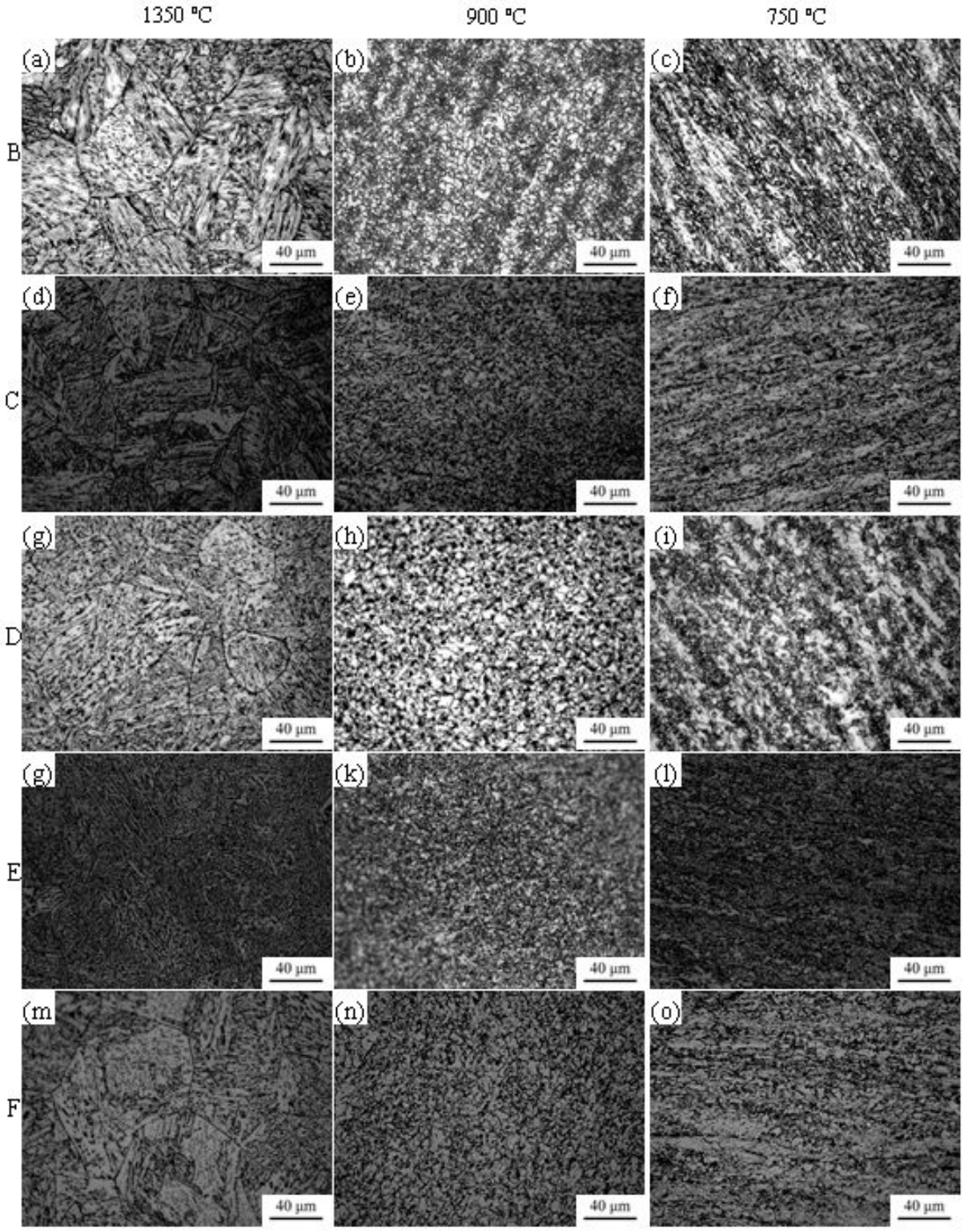

Figure 5. Optical metallographs of the test steels at different simulated peak temperature: Steel B: (a) 1350 °C; (b) 900 °C; (c) 750 °C; Steel C: (d) 1350 °C; (e) 900 °C; (f) 750 °C; Steel D: (g) 1350 °C; (h) 900 °C; (i) 750 °C; Steel E: (j) 1350 °C; (k) 900 °C; (l) 750 °C; Steel F: (m) 1350 °C; (n) 900 °C; (o) 750 °C.

The base metal microstructure of Steel A is the mixed microstructure of fine AF and BF, and the microstructure maintains the ribbon characteristics formed by elongation of the primary austenite grain with the low temperature controlled rolling (Figure 2a). After the weld thermal cycle, the microstructure changed obviously. When the peak temperature is 1350 °C, the

microstructure is the typical GB and show the typical characteristic of the coarse grained heat affected zone. Coarse primary austenite grain boundary is clearly visible. The GB is composed of banite, a small amount of MF, and lamellate islands in banite laths, as well as the islands distributed freely on MF (Figure 3a). TEM analysis shows that the island structure is M/A constituent, BF and MF possess high dislocation density, and BF has smaller orientation difference and larger effective grain size (orientation difference≥15°) (Figure 4a). Which is confirmed in the results of EBSD, as shown in Figure 6a, the primary austenite grain boundary belongs to large angle grain boundary, while the structures inside the austenite grains mainly consist of small angle grains, and the effective grain size is about 8.5 μm (Figure 6a).

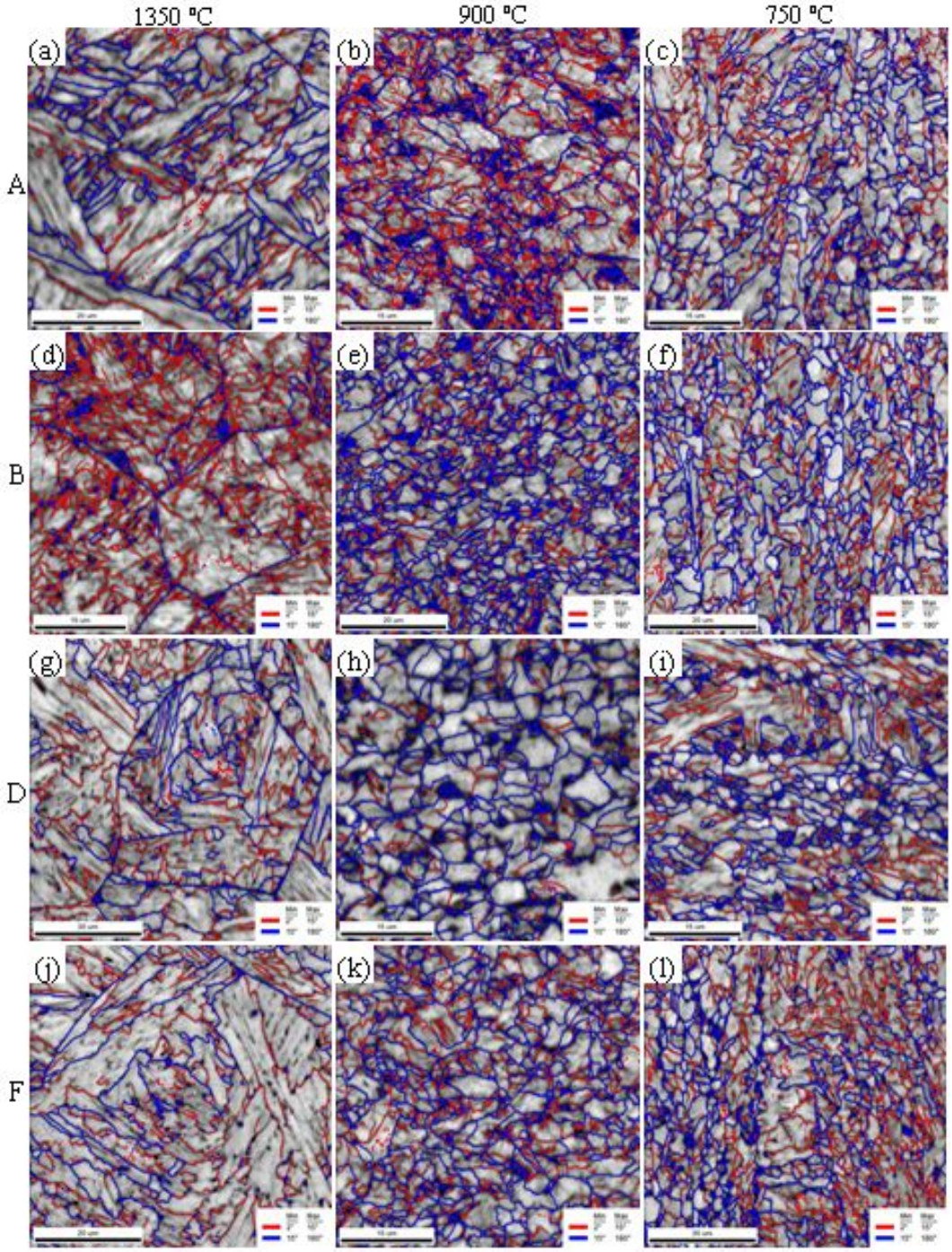

Figure 6. EBSD analysis of the simulated test steels at different simulated peak temperature: Stell A: (a) 1350 °C; (b) 900 °C; (c) 750 °C; Steel B: (d) 1350 °C; (e) 900 °C; (f) 750 °C; Steel D: (g) 1350 °C; (h) 900 °C; (i) 750 °C; Steel F: (j) 1350 °C; (k) 900 °C; (l) 750 °C.

Table 2. The classifications of microstructure in low-carbon microalloyed steels.

Microstructure	acronym
polygonal ferrite	PF
quasi-polygonal ferrite	QF
massive ferrite	MF
granular bainite	GB
Bainite ferrite	BF
acicular ferrite	AF
martensite/austenite	M/A
granular ferrite	GF

When the temperature decreases to 1200 °C, the microstructure is still appear GB structure, but the primary austenite grain size decrease obviously, the characteristics of lath like structure is abate, M/A islands constituent distributed in matrix mainly present dot or stich like. As the peak temperature decrease below 900 °C, the microstructure has a great change, the primary austenite grain boundary disappears, and the microstructure is consist of GF, AF and a little PF (Figure 3d). GF grain boundary is irregular and a large number of dislocation remains in its interior (Figure 4b). EBSD analysis showed that the grain size is mainly large angle grain boundary, and the effective grain size significantly reduces, which is approximately 7.5 μm (Figure 6b). When the peak temperature is 800 °C, the microstructure presents a mixture characteristics of ferrite and island constituent, partial austenitizing structure transformation during cooling because of the peak temperature is in the two-phase critical region, at the same time, as the original rolling state acicular ferrite and bainite tempering transformation, the area still retains the characteristics of strip rolling characteristics (Figure 3e). The TEM analysis showed that the island constituent is bainite or M/A constituent with high density dislocation (Figure 4c). EBSD analysis results also confirmed that the darker portion in metallographic is made up of fine large angle grain, and there is a small number of small angle subboundary existence in ferrite, the average effective grain size is 7.1 μm (Figure 6c).

The variations of microstructure in other test steels are similar to that of Steel A, but with the increase of Cu, Cr or Mo content in steel, the effective grain size decreases while the proportion of large angular grain boundary increases. In addition, BF content increases while GB content decreases in the CGHAZ, GB and AF content increase and PF content decreases in the FGHAZ. It can be seen that the increase of Cu, Cr or Mo content in X90 steel also has a great impact on microstructure.

For X90 steel, after the welding thermal cycle, it not only shows the embrittlement caused by the reduction of toughness, but also shows the softening caused by the reduction of strength. Embrittlement area appeared in the peak temperature of 1350 °C and 750 °C, While the strength softening zone appeared when the peak temperature within the range of 900-1000 °C (Figure 1). From the microstructure, when the peak temperature within the range of 1350 ~ 1200 °C, the microstructure at room temperature is GB, and the primary austenite grain boundary is clearly visible. With the temperature decrease to 1000~900 °C range, the microstructure at room temperature is fine GF. When the temperature decreased below 800 °C, the microstructure is consistent of PF and GB, and still remain the zonal characteristics that is similar to rolling state. This microstructure variation changed by rapid heating, cooling and heating temperature during welding thermal cycle.

Based on Hutchinson et al. [7], calculated by the composition of steel, the phase transition temperature during heating process (Ac1 and Ac3) of the test steels are as shown in Table 3, which is about 700 °C and 830 °C, respectively. However, under the condition of rapid heating, phase transformation temperature is significantly increased [16], by the expansion method determining the Ac1 and Ac3 of the test steels are shown in Table 3, which is about 730 °C and 925 °C, respectively, i.e., the steels were austenitized completely when the temperature is higher than 925 °C. The peak temperature affects the degree, state and grain size of austenite crystallization, and thus significantly affects the phase transition during the cooling process, ultimately affecting the microstructure and properties at room temperature. Figure 7 shows the effect of different peak temperatures on the starting temperature of phase transition during the cooling process (Ar3).

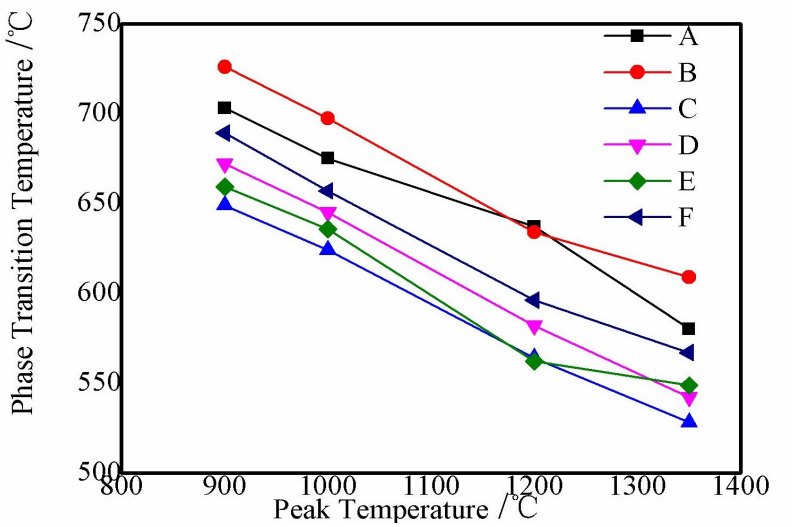

Figure 7. The phase transition temperature during cooling at different simulated peak temperatures of the test steels (Ar3).

The Ar3 increases with the peak temperature decrease from 1350 °C to 900 °C. But when the peak temperature is below 900 °C, it is difficult to determine the phase transition temperature during cooling from the expansion curve. The different austenite states and cooling transformations have great influences on the microstructure and properties after cooling.

When the peak temperature is below 700 °C, austenitization has not occurred yet, in the process of thermal cycle, the acicular ferrite obtained after controlled rolling and controlled cooling was tempered, it is widely believed that the strength should decrease and toughness should increase on this occasion [16]. But for low carbon high Nb micro alloyed steel, there is a large amount of Nb solid solution precipitating and strengthening in the process of thermal cycling [17] after controlled rolling and controlled cooling, and then improving the strength and toughness of steel with the increase of tempering temperature (Figure 1). When the peak temperature gets to 750 °C, which has just entered the two-phase region, a small amount of austenite forms on the primary austenite grain boundry or bainite boundary and close to M/A island, and formed bainite or M/A island constituents with high strength and low toughness during cooling (Figure 1), led to toughness deteriorate sharply [14] (Figure 1). With the further increase of the peak temperature, the amount of austenite transition and the degree of matrix tempering increase. The number of bainite or M/A island constituents obtained by austenite in the cooling process decreased, and a large number of PF and GF appeared (Figure 2 and Figure 3), so the strength decreased, but the toughness improved (Figure 1). When peak temperature reaches 900 °C, the microstructure has been basically austenitizing completely, but due to the nonuniformity of austenite and a large number of tiny Nb (CN) precipitation hold-up the austenitic grain growth, the phase transformation temperature is higher during cooling (Figure 6), and the microstructure is fine PF and GF (Figure 2-5), toughness have been improved significantly, but the strength is lower (Figure 1). When the peak temperature increases higher than 1000 °C, austenitizing has proceeded completely, the austenitic grain began to grow up, the hardenability of steel are rising and the phase transition temperature is reduced, the amount of GB increases after cooling, thus obtains higher strength but lower toughness (Figure 1). For high Nb steel, Nb (CN) fast dissolving temperature is above 1150 °C [18], therefore, when the peak temperature is above 1200 °C, the austenitic grains begin to rapidly grow up (Figure 3), phase transition temperature significantly decreases (Figure 6), the microstructure changes to GB, the toughness decreases further, and the strength increases. By the austenitic grain size, at 1350 °C, the primary austenite grain size remained about 60 μm (Figure 1), and toughness decreased significantly, which is related to the larger effective grain size in GB obtained after cooling (Figure 3).

The microstructures at room temperature in different HAZ region of the six test steels is different, due to the different peak temperature in welding thermal cycle and different phase transition temperature during cooling. While, the difference in constitution and distribution of microstructure made a considerable influence on strength and toughness, that is, at different peak temperatures, the phase transition temperature has a big effect on strength and toughness. The grain size of primary austenite affects the transition temperature of supercooled austenite in a certain extent [19]. The fine austenitic grain and high grain boundary density is benefit of ferrite nucleation in the austenite grain boundary, in the HAZ microstructure of X90 pipeline steels, the smaller the grain boundary, the less its dislocation, the smaller the difference of strain at grain boundaries, sequentially the smaller the stress concentration caused by dislocation pile-up in the grain boundary, and the greater the stress required for plastic deformation during neighboring grain, i.e. the higher the yield strength [20]. At the same time, the amounts of the element atoms and fine second phase increase with the grain boundary increase, and its effect on inhibiting dislocation movement is enhanced. The increase of alloy elements will increase the content of solid solution precipitation in the matrix, thus reducing the effective grains size, and increasing the strength and toughness of in HAZ (Figure 1). In HAZ, the

high temperature will accelerate the dissolution of the original precipitate and make the grain coarse severely, which is not conducive to the grain nucleation. Phase change temperature also decreases because of part of the precipitate particles dissolving and the element content of solid solution increasing, which is advantageous to the formation of low temperature microstructure, as a result, in the CGHAZ, the contents of BF in Steel B, D, E are higher than that in Steel A, B, C, respectively, and in the FGHAZ, the contents of GB and AF are higher than that in Steel A, B, C, respectively. GB constituent compared with BF constituent, or GB and AF constituents compared with PF and QF constituents, the laths are finer, dislocation density is bigger, M/A island constituent present acicular and its distribution is more dispersed, and the proportion of the large angle grain boundary is bigger. The large angle grain boundary can improve toughness by changing the directions of dislocation slip and crack propagation [21], meanwhile, the fine and dispersed M/A constituents are also conducive to obtaining higher impact energy. Therefore, the increase of alloy elements will increase the proportion of large angle grain boundary, at the same time, the higher density dislocation and smaller dispersed M/A elements can be obtained, thus improving the strength and toughness of HAZ.

In conclusion, there are distinguishing brittlement and softening characteristics in the welding heat affected zone of X90 high-strength pipeline steels. According to the study of X80, reasonable composition design can improve the characteristics of brittlement and softening [14]. Therefore, the study of high strength pipeline steel, in composition design, combined the technology of welding process, should not only attach importance to the toughness of welding heat affected area, but also should pay attention to softening caused by strength of heat affected zone.

Table 3. The Ac1 and Ac3 values of the test steels (°C).

	Steel A	Steel B	Steel C	Steel D	Steel E	Steel F
Ac1(°C) Calculated value	695	696	690	695	694	693
Ac3(°C) Calculated value	836	836	842	830	829	828
Ac1(°C) Measured value	725	730	728	729	729	730
Ac3(°C) Measured value	922	927	920	925	925	928

4. Conclusions

(1) The embrittlement zone appears in the ICHAZ when the peak temperature was at 750 °C and CGHAZ when the peak temperature was above 1200 °C. The embrittlement in ICHAZ at 750 °C was caused by brittle bainite and M /A islands formed during cooling, because little austenite was formed during heating. While, the embrittlement in CGHAZ is caused by austenite grain coarsen, which transformed to the coarse bainite after cooling;

(2) The softening area appears at the junction of the ICHAZ and the FGHAZ when the peak temperature was in the range of 900-1000 °C. The softening zone attributed to the polygonal ferrite and granular ferrite after cooling, which came from fine and ununiform austenite formed during reheating process;

(3) Ar3 of HAZ in X90 pipeline steels decreases with the peak temperature increasing. The peak temperature greatly affects the austenitizing and its grain size, thereby affects phase transition during cooling process, and ultimately affects its microstructure and properties at room temperature;

(4) With the increase of Cu, Cr or Mo content in steels, Ar3 decreases and the BF content in CGHAZ, GB and AF content in FGHAZ increase, therefore the strength and toughness of HAZ increase.

Acknowledgements

This paper is supported by National Natural Science Foundation of China (51671164) and Hebei Natural Science Fund -- steel joint fund (E2015203234).

References

[1] Idris R, Prawoto Y. Influence of ferrite fraction within martensite matrix on fatigue crack propagation: an experimental verification with dual phase steel. Materials Science and Engineering A. 2012;552:547-554. http://dx.doi.org/10.1016/j.msea.2012.05.085.

[2] Aydin H, Nelson TW. Microstructure and mechanical properties of hard zone in friction stir welded X80pipeline steel relative to different heat input. Materials Science and Engineering A. 2014;586:313-322. http://dx.doi.org/10.1016/j.msea.2013.07.090.

[3] Yan CY, Liu CY, Yan B. 3D modeling of the hydrogen distribution in X80 pipeline steel welded joints. Computational Materials Science. 2014;83:158-163. http://dx.doi.org/10.1016/j.commatsci.2013.11.007.

[4] Frantov II, Velichko AA, Bortsov AN, Utkin IY. Weldability of niobium-containing high-strength steel for pipelines welding research. Welding Journal. 2014;93:23-29.

[5] Wang LW, Liu ZY, Cui ZY, Du CW, Wang XH, Li XG. In situ corrosion characterization of simulated weld heat affected zone on API X80 pipeline steel. Corrosion Science. 2014;85:401-410. http://dx.doi.org/10.1016/j.corsci.2014.04.053.

[6] Sowards JW, Gnäupel-Herold T, David McColskey J, Pereira VF, Ramirez AJ. Characterization of mechanical properties, fatigue-crack propagation, and residual stresses in a microalloyed pipeline-steel friction-stir weld. Materials & Design. 2015;88:632-642. http://dx.doi.org/10.1016/j.matdes.2015.09.049.

[7] Hutchinson B, Komenda J, Rohrer GS, Beladi H. Heat affected zone microstructures and their influence on toughness in two microalloyed HSLA steels. Acta Materialia. 2015;97:380-391. http://dx.doi.org/10.1016/j.actamat.2015.05.055.

[8] Qi LH, Jin ZL, Zhang JM, Wang YL, Hu MJ, Wang ZC. Influence factors of X70 pipeline steel girth welding with self-shielded flux-cored wire. Materials Science and Technology. 2017;33(5):592-601. http://dx.doi.org/10.1080/02670836.2016.1238646.

[9] Cheng AK, Chen NZ. An extended engineering critical assessment for corrosion fatigue of subsea pipelin steels. Engineering Failure Analysis. 2018;84:262-275. http://dx.doi.org/10.1016/j.engfailanal.2017.11.012.

[10] Li HJ, Liang L, Feng YL, Huo D-X. Microstructure transformation of X70 pipelinesteel welding heat-affected zone. Rare Metals. 2014;33(4):493-498. http://dx.doi.org/10.1007/s12598-014-0344-x.

[11] Kong X, Qiu C. Continuous cooling bainite transformation characteristics of a lowcarbon microalloyed steel under the simulated welding thermal cycle process. Journal of Materials Science and Technology. 2013;29(5):446-450. http://dx.doi.org/10.1016/j.jmst.2013.03.022.

[12] Yue X. Investigation on heat-affected zone hydrogen-induced cracking of highstrengthnaval steels using the Granjon implant test. Welding in the World. 2015;59(1):77-89. http://dx.doi.org/10.1007/s40194-014-0181-4.

[13] Kumar S, Nath SK, Kumar V. Continuous cooling transformation behavior in the weld coarse grainedheat affected zone and mechanical properties of Nb-microalloyed andHY85 steels. Materials & Design. 2016;90:177-184. http://dx.doi.org/10.1016/j.matdes.2015.10.071.

[14] Chen XW, Liao B, Qiao GY, Gu Y, Wang X, Xiao F. Effect of Nb on mechanical properties of HAZ for high-Nb X80 pipeline steels. Journal of Iron and Steel Research International. 2013;20(12):53-60. http://dx.doi.org/10.1016/S1006-706X(13)60216-2.

[15] Zhao ZP, Qiao GY, Li GP, Yang W-W, Liao B, Xiao F-R. Fatigue properties of ferrite/bainite dual-phase X80 pipeline steel welded joints. Science and Technology of Welding and Joining. 2017;3(3):217-226. http://dx.doi.org/10.1080/13621718.2016.1219120.

[16] Mohanty RR, Girina OA, Fonstein N. Effect of heating rate on the austenite formationin low-carbon high-strength steels annealed in the intercritical region. The Minerals. Metals & Materials Society. 2011;42:3680-3690.

[17] Xiao F, Cao Y, Qiao G, Zhang X, Liao B. Quantitative research on effectiveness of Nb solute and NbC precipitates on dynamic or static recrystallization in Nb steels. Journal of Iron and Steel Research International. 2012;19(11):52-56. http://dx.doi.org/10.1016/S1006-706X(13)60020-5.

[18] Gu Y, Tian P, Wang X, Han X, Liao B, Xiao F. Non-isothermal prior austenite grain of a high-Nb X100 pipeline steel during a simulated welding heat cycle process. Materials & Design. 2016;89:589-596. http://dx.doi.org/10.1016/j.matdes.2015.09.039.

[19] Lambert-Perlade A, Gourgues AF, Besson J, Sturel T, Pineau A. Mechanisms and modeling of cleavage fracture in simulated heat-affected zone microstructures of A high-strength low alloy steel. Metallurgical and Materials Transactions. A, Physical Metallurgy and Materials Science. 2004;35(13):1039-1053. http://dx.doi.org/10.1007/s11661-004-1007-6.

[20] Wan XL, Wu KM, Huang G, Wei R, Cheng L. In situ observation of austenite grain growth behavior in the simulated coarse-grained heat-affected zone of Ti-microalloyed steels. International Journal of Minerals Metallurgy and Materials. 2014;21(9):878-885. http://dx.doi.org/10.1007/s12613-014-0984-8.

[21] Kejian H, Baker TN. The effects of small titanium additions on the mechanical properties and the microstructures of controlled rolled niobium-bearing HSLA plate steels. Materials Science and Engineering A. 1993;169(1-2):53-56. http://dx.doi.org/10.1016/0921-5093(93)90598-9.